International Journal of Microwave and Wireless Technologies

cambridge.org/mrf

Strong coupling induced notched bands of UWB antennas using meta-surfaces

Jinbiao Zhu[1,2], Wen Jiang[1], Yuquan Liu[2], Pengyu Yin[2] and Lili Guo[2]

[1]Northwestern Polytechnical University, Xi'an, China and [2]Aerospace Information Research Institute, Chinese Academy of Sciences, Beijing 100094, China

Research Paper

Cite this article: Zhu J, Jiang W, Liu Y, Yin P, Guo L (2023). Strong coupling induced notched bands of UWB antennas using meta-surfaces. *International Journal of Microwave and Wireless Technologies* **15**, 843–851. https://doi.org/10.1017/S1759078722000873

Received: 28 December 2021
Revised: 10 July 2022
Accepted: 11 July 2022

Key words:
Band-notched antenna; coupling effects; meta-surfaces; reconfigurable; ultra-wideband antennas

Author for correspondence:
Wen Jiang,
E-mail: jiangwen@nwpu.edu.cn

Abstract

The meta-surface is introduced into the design of band-notched monopole antennas with single/dual/triple notched bands around 3.6/5.5/7.2 GHz for ultra-wideband (UWB) communication. We show that strong coupling effects between the meta-surface and the antenna would be created through tuning the orientations of the meta-cells according to the field distributions on the antenna surface, and eventually, filter the unwanted radiations of the antenna. Especially, by simply attaching different meta-surfaces on the back of the antenna, the band-notched properties are shown to be changeable without hurting the original structure of the antenna. Both simulation and measurement results demonstrate the monopole with replaceable meta-surfaces has achieved an UWB operating band ranging from 3 to 9 GHz for voltage standing wave ratio (VSWR) ≤ 2 with single/dual/triple notched bands covering frequencies around 3.6/5.5/7.2 GHz. Such a design would obtain significant notched performances for the desired bands and maintain the good radiations in the operating frequency, which make it a suitable candidate for UWB applications.

Introduction

The band-notched design has become a very popular research area in the antenna engineering with the aim to filter and suppress the interferences that degrade the overall performances of the electromagnetic system. Among all the band-notched antenna designs, the trapping wave technology using notched structures has widely been employed in such a research area for its simple design and efficiency. Such a strategy generally uses specific etched or printed resonant structures to obtain the desired band-notched performances, through carving slots [1–5], adding parasitic elements [6–13], appending matching stubs [14–16] on the original antennas, thus offers very practical solutions to the band-notched antenna designs. In addition, carving tapered-shape slot in the ground plane [17] or using partial ground plane [18] can influence the coupling between the patch and the ground plane, thus enhances the operating bandwidths of the ultra-wideband (UWB) antenna.

Meta-surface, as a new kind of artificial materials, has demonstrated the great capacity of controlling electromagnetic fields. Especially, the meta-surfaces have been used to manipulate the interactions between the neighboring radiating components of the antennas, where periodic complementary split ring resonator [19, 20], folded split ring resonators (SRRs) [21], and electromagnetic band gap (EBG) [22, 23] demonstrated the functionalities of reducing the coupling between patch antennas. In this paper, we propose to use replaceable meta-surfaces to implement the band-notched UWB monopole and vivaldi antennas. We show that strong coupling effects between the meta-surface and the antenna would be created through tuning the orientations on the meta-cell according to the field distributions on the antenna surface, and eventually, filter the unwanted radiations of the antenna. Especially, by simply attaching different meta-surfaces on the back of the antenna, the band-notched properties are shown to be changeable without compromising the original structure of the antenna. Such antenna can obtain notched performances for the desired bands, while maintaining the good radiations at the un-notched frequencies, hence is suitable for UWB wireless communication applications. This paper is organized as follows: section "Antenna design and simulation resulta" introduces the configuration of the antennas and meta-surfaces. Full-wave simulations and the operating mechanism of the antennas are illustrated by presenting reconfigurable band-notched designs. In section "Fabrications and experimental results", we carry out the experiments to verify our proposed designs, and finally, conclusions are drawn in section "Conclusion".

Antenna design and simulation results

Let us start with the dual-band notched monopole antenna design. The configuration of the antennas and the corresponding meta-surfaces are demonstrated in Fig. 1. The UWB

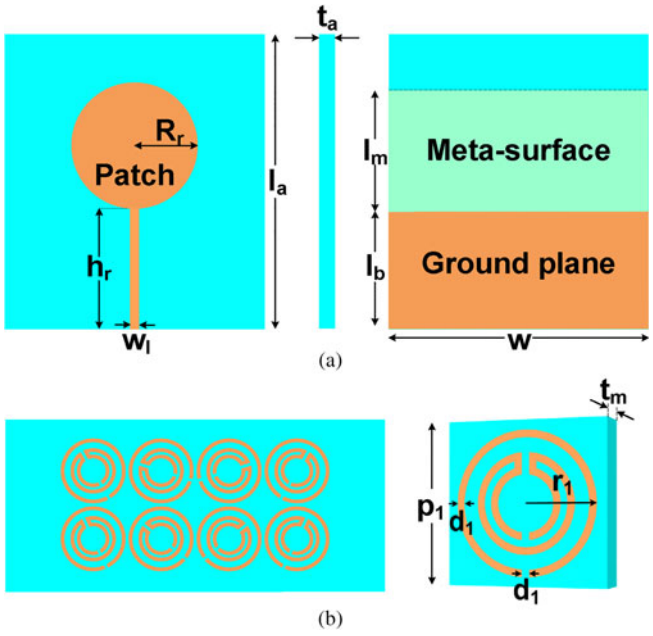

Fig. 1. Configuration of the dual-band notched monopole antenna. (a) Original UWB monopole antenna. (b) The dual-band notched meta-surface and the unit cell.

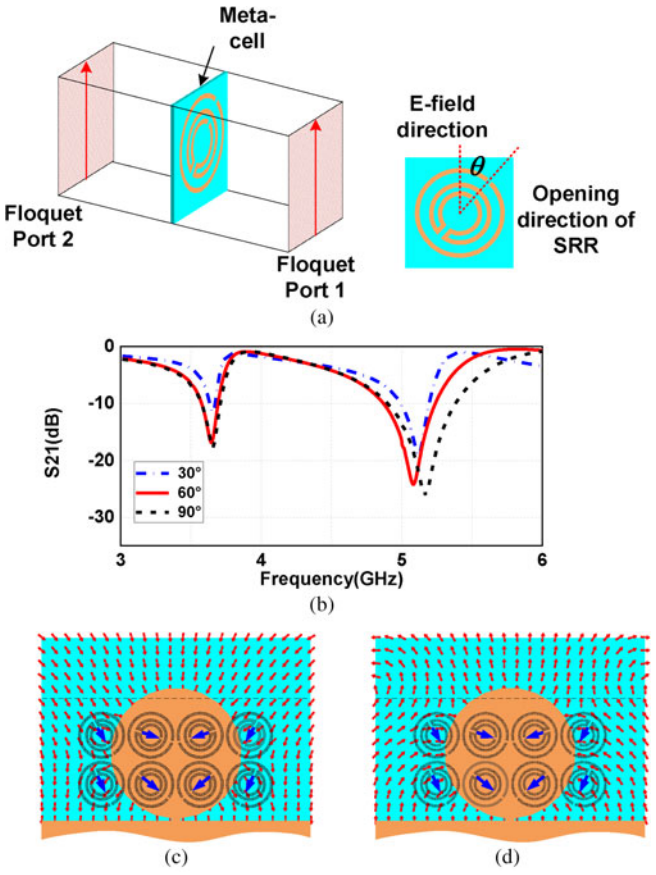

Fig. 2. Design of dual-band notched meta-surface. (a) Simulation *M*odel and (b) the transmission coefficients of dual-band notched meta-surfaces with different oriented meta-cells. E-field distributions on the surface of the planar monopole antenna disc at (c) 3.6 GHz, and (d) 5.1 GHz.

monopole antenna employed here would have a broadband operating frequency from 3 to 9 GHz. The structural parameters of the monopole antenna are $w = 44$ mm, $w_l = 1.4$ mm, $l_a = 50$ mm, $l_b = 20$ mm, $l_m = 20$ mm, $R_r = 10.7$ mm, $h_r = 20.4$ mm, $r_1 = 3.7$ mm, $d_1 = 0.4$ mm, $t_a = 0.6$ mm, $t_m = 0.1$ mm, and the period of meta-cell is $p_1 = 8$ mm with the radius of 2.65 and 1.9 mm for the composite ring. It is fabricated on the FR4 substrate with $\varepsilon_r = 4.4$ and the loss tangent of 0.02. We intend to attach a meta-surface on the bottom side of the monopole antenna to generate a dual-band notched filtering radiations through strong coupling effects instead of conventional strategy of directly etching the radiation patch or the antenna ground plane. In this way, we can implement reconfigurable band-notched properties of the monopole by simply replacing different meta-surfaces.

The meta-cells on meta-surface are chosen as the SRRs with the resonant frequency simply tuned through the SRR perimeter [24, 25]:

$$f \approx \frac{c}{2 \times L_{tol} \times \sqrt{\varepsilon_{eff}}} \tag{1}$$

where f refers to the resonant frequency, c refers to the speed of light in vacuum, L_{tol} refers to SRR perimeter, ε_{eff} refers to the effective permittivity of dielectric substrate and surrounding air. The dual-band notched meta-surface in Fig. 1 consists of eight identical structural SRRs with different orientations fabricated on a 0.1 mm thick FR4 substrate. To create a notched band centered at 3.6 GHz, the inner-ring of the SRRs was extended inwards to form a composite ring structure and the outer-ring of the SRRs creates a notched band centered around 5.1 GHz. By adjusting the total length of the inner and outer rings, the dual-band notched characteristic of the meta-surface can be adjusted separately.

However, the resonance behaviors of the meta-cell are sensitive to the SRR orientations in relative to the direction of the E-fields [26] and thus, we would better optimize the rotating angles of SRRs to obtain the best coupling effects when integrated with the monopole antenna. To be more specific, the resonance responses of SRRs would be strongest when the direction of the E-field is perpendicular to the split. In addition, such resonance responses are shown to be different as the operating frequency changes. We can observe in Fig. 2 that electromagnetic fields with more than 60-degree incident angels would create almost the same resonance intensity in the lower frequency, while 60-degree and 90-degree incidences beyond 5 GHz would perform differently. With such resonant behaviors of the employed SRRs, we carefully arrange the orientation of the meta-cells according to the E-field distributions of the monopole antenna at 3.6 and 5.1 GHz to let the orientation of splits exactly perpendicular to the E-fields at 5.1 GHz, and can also maintain larger than 60-degree at 3.6 GHz to achieve the best coupling for the desired band-notched performance.

To investigate the dual-band notched behavior of the proposed meta-surface, an equivalent LC circuit model is proposed in Fig. 3. The representation of an antenna as a lumped-element circuit with two parallel RLC resonators, where the first resonator is designed to operate around 3.3 GHz and the second around 5.15 GHz. The equivalent model calculates the quality factor (Q_0) of the notched bands. The circuit also provides the concept of modeling the distributed element into its corresponding equivalent lumped entities. The values of the lumped elements calculation

https://doi.org/10.1017/S1759078722000873 Published online by Cambridge University Press

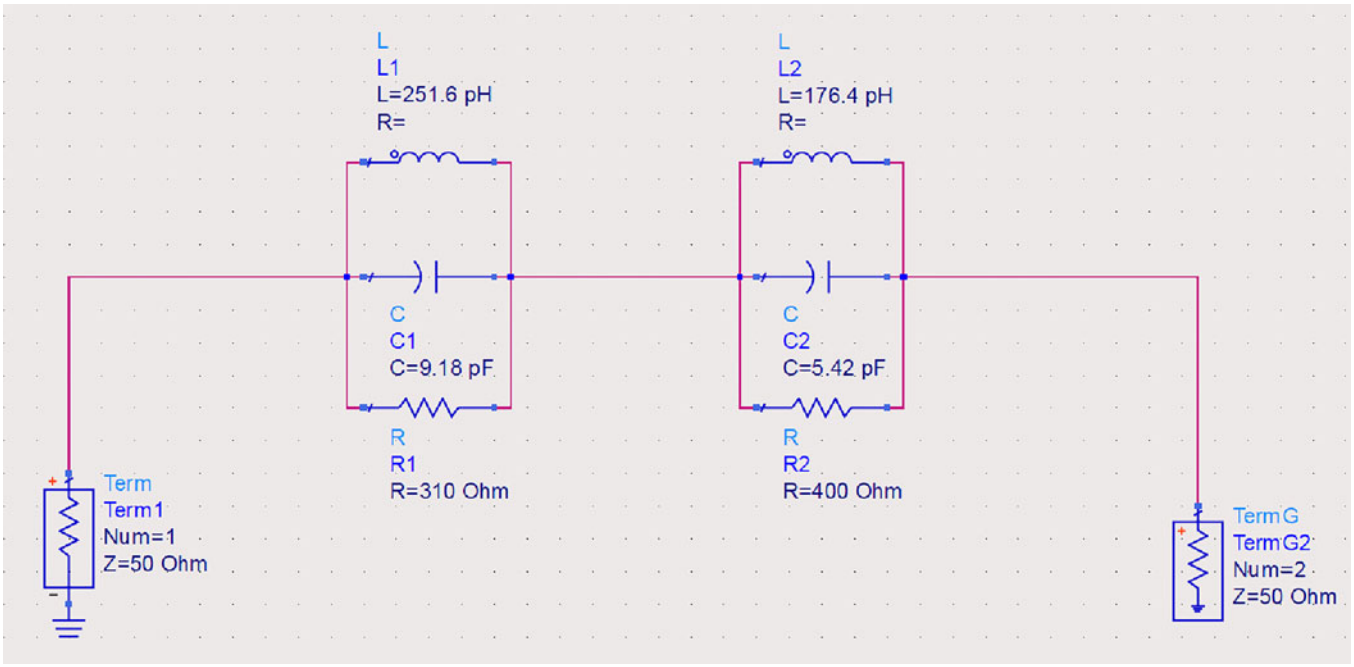

Fig. 3. The LC resonant circuit model of proposed dual-band notched meta-surface.

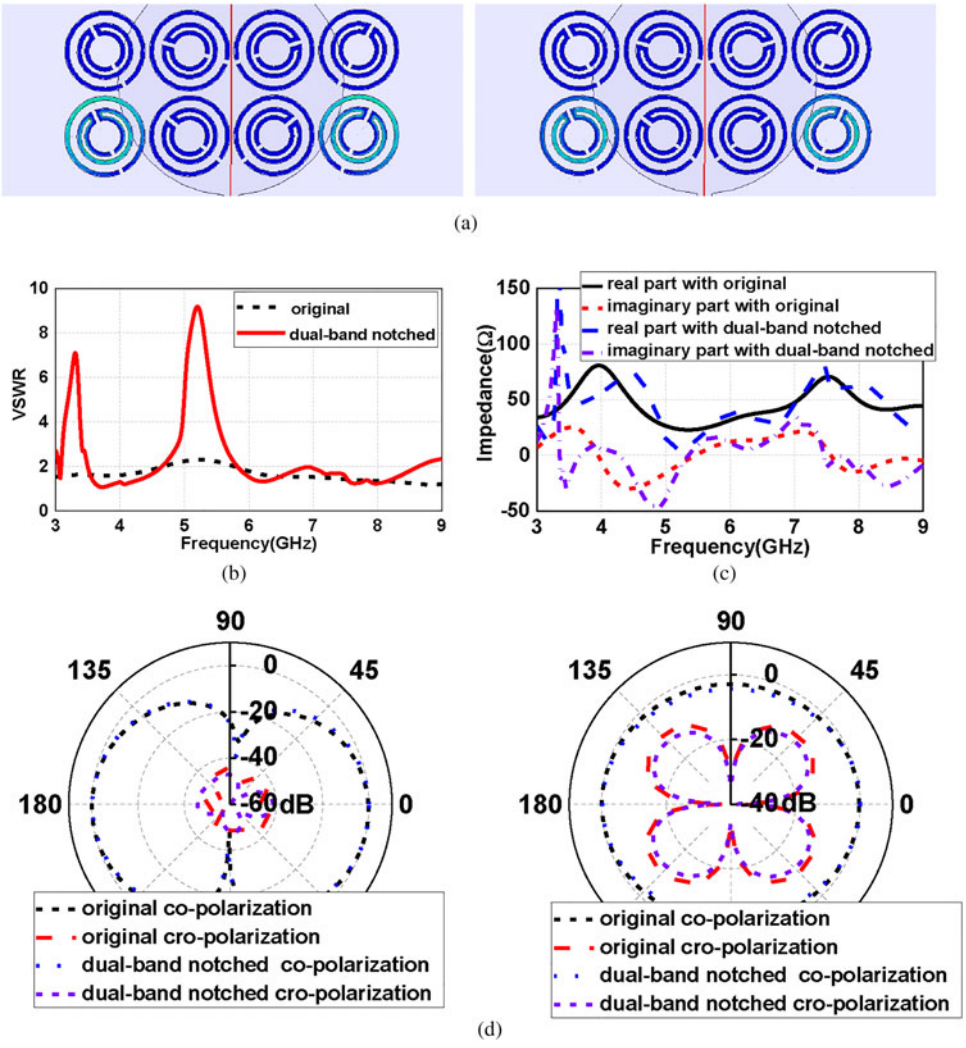

Fig. 4. Simulation results of dual-band notched monopole antenna. (a) Surface current distributions of the SRRs, where the left is the frequency at 3.3 GHz and the right is the frequency at 5.15 GHz. (b) VSWR and (c) real and imaginary parts of the monopole antenna with and without the meta-surfaces. (d) Normalized E-plane (left) and H-plane (right) radiation patterns of dual-band notched monopole antenna at 4.5 GHz.

https://doi.org/10.1017/S1759078722000873 Published online by Cambridge University Press

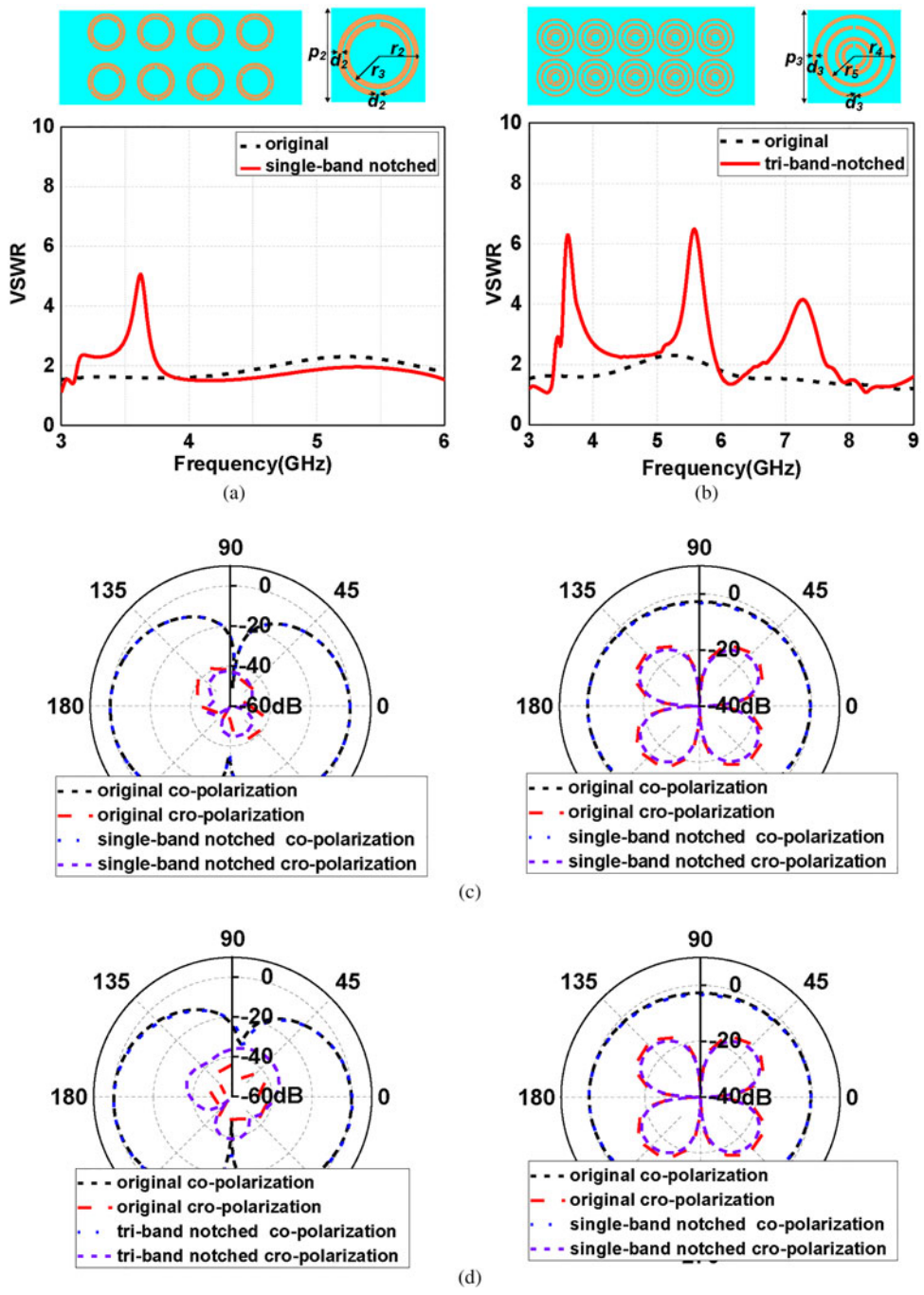

Fig. 5. Simulation results for single-band and tri-band notched monopole antenna. VSWR of monopole antennas with (a) single-band notched mate-surface, (b) tri-band notched meta-surface. Simulated E-plane (left) and H-plane (right) radiation patterns of monopole antennas with (c) single-band notched meta-surface at 4 GHz, and (d) tri-band notched meta-surface at 4.5 GHz.

are carried out using the following equations [27, 28]:

$$Q_0 = \frac{f}{BW}, \quad Q_0 = 2\pi f_0 RC, f_0 = \frac{1}{2\pi\sqrt{LC}}, \tag{2}$$

where f_0 is the resonant notched frequency, R is the resistor, L is the inductor, C is the capacitor of RLC circuit. For the dual-band notched antenna, the values of the lumped elements are $L_1 =$ 251.6 nH, $C_1 = 9.18$ pF, $R_1 = 310\ \Omega$, $L_2 = 176.4$ nH, $C_2 = 5.42$ pF, $R_1 = 400\ \Omega$, .

The full-wave simulation (Ansoft HFSS v.18.0) is carried out to verify our design in Fig. 4. We can observe that VSWR of the monopole antenna loaded with meta-surface would have the dual-band notched radiations around 3.3 and 5.15 GHz as we devised, while the antenna without the meta-surface would operate smoothly over the wide frequency range from 3 to 9 GHz. Figure 4(a) demonstrates the surface current distributions of the SRRs and we can observe that both inner- and outer-rings resonate at 3.3 GHz while only the inner-ring resonates at 5.5 GHz. Thus we can adjust the length of the inner-ring to control the

https://doi.org/10.1017/S1759078722000873 Published online by Cambridge University Press

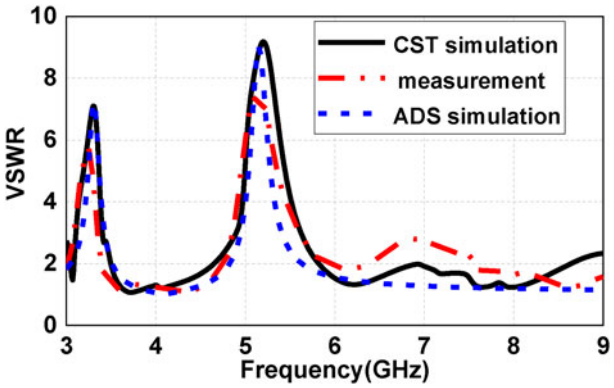

Fig. 6. The VSWRs of the circuit model, simulation, and measurement for the dual-band notched antenna.

band-notched characteristics at high frequency and change the length of the inner- and outer-rings to control the band-notched characteristics at low frequency. The real and imaginary parts of the input impedance of the presented antenna with and without meta-surface are shown in Fig. 4(c). We can observe that the real and imaginary parts of the input impedance of the antenna without notch bands are close to 50 and 0 characteristic line and demonstrate a good impedance matching resulting in a ultra-wide operating band. On the other hand, at around 3.3 and 5.15 GHz the real and imaginary parts of the input impedance of the antenna with notch bands are, respectively, much away from 50 and 0 characteristic line and exhibit higher impedances resulting in a mismatching. Due to this mismatching, two notch bands are created at around 3.3 and 5.15 GHz. We continue to demonstrate the radiation performances at the frequency between the two notched frequencies in order to examine whether such a meta-surface would influence the radiation performance of the original monopole antenna. We can observe that the radiation patterns are fairly good omnidirectional in H-plane and dumbbell-shaped in E-plane. Clearly, the radiation patterns at un-notched frequencies are scarcely deteriorated when meta-surface is added.

Based on the same strategy, we extend our design into the single-band and tri-band notched monopole antenna by using the corresponding meta-surfaces, as shown in Fig. 5. For single-band notched meta-surface, the SRR with two rings has been used to create a notched band around 3.6 GHz. Compared to the dual-band notched meta-surface, the tri-band notched meta-surface has three resonant rings. In order to keep the period of the meta-cell unchanged, the width of the resonant ring is reduced from 0.4 to 0.3 mm. We placed the single-band notched meta-surface consisting of eight SRRs with the structural parameters of $p_2 = 9$ mm, $r_2 = 3.5$ mm, $r_3 = 2.8$ mm, $d_2 = 0.4$ mm and tri-band notched meta-surface consisting of 10 SRRs with the structural parameters of $p_3 = 8$ mm, $r_4 = 3.78$ mm, $r_5 = 2.78$ mm, $d_3 = 0.3$ mm and the radius of composite ring as 1.73 and 1.13 mm to implement the single-band and tri-band notched monopole antenna. Simulation results indicated that single-band notched frequency occurred around 3.58 GHz and tri-band notched frequencies occurred around 3.57, 5.55, and 7.18 GHz. In addition, the radiation patterns of the single-band and tri-band notched monopole antenna at un-notched frequencies are scarcely deteriorating when meta-surfaces are added.

Fabrications and experimental results

To verify the proposed designs, the monopole antenna and three different meta-surfaces are fabricated and measured. Figure 6 shows that the VSWRs of the circuit model, simulation and measurement results for the dual-band notched antenna and all results remain highly consistent. Figure 7 shows that VSWR of band-notched monopole antennas respectively presents single-band, dual-band, and tri-band notched characteristic compared with the VSWR of monopole without meta-surface, which match

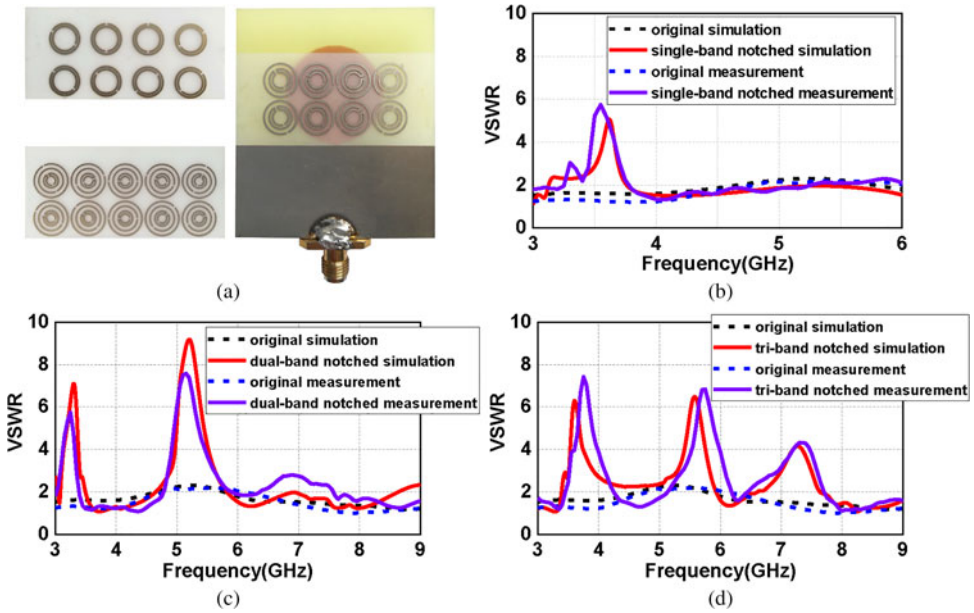

Fig. 7. Band-notched monopole antenna and measurement results. (a) Photographs of the manufactured monopole antenna and meta-surfaces. Measured VSWR of monopole antenna with (b) single-band notched meta-surface, (c) dual-band notched meta-surface, and (d) tri-band notched meta-surface.

https://doi.org/10.1017/S1759078722000873 Published online by Cambridge University Press

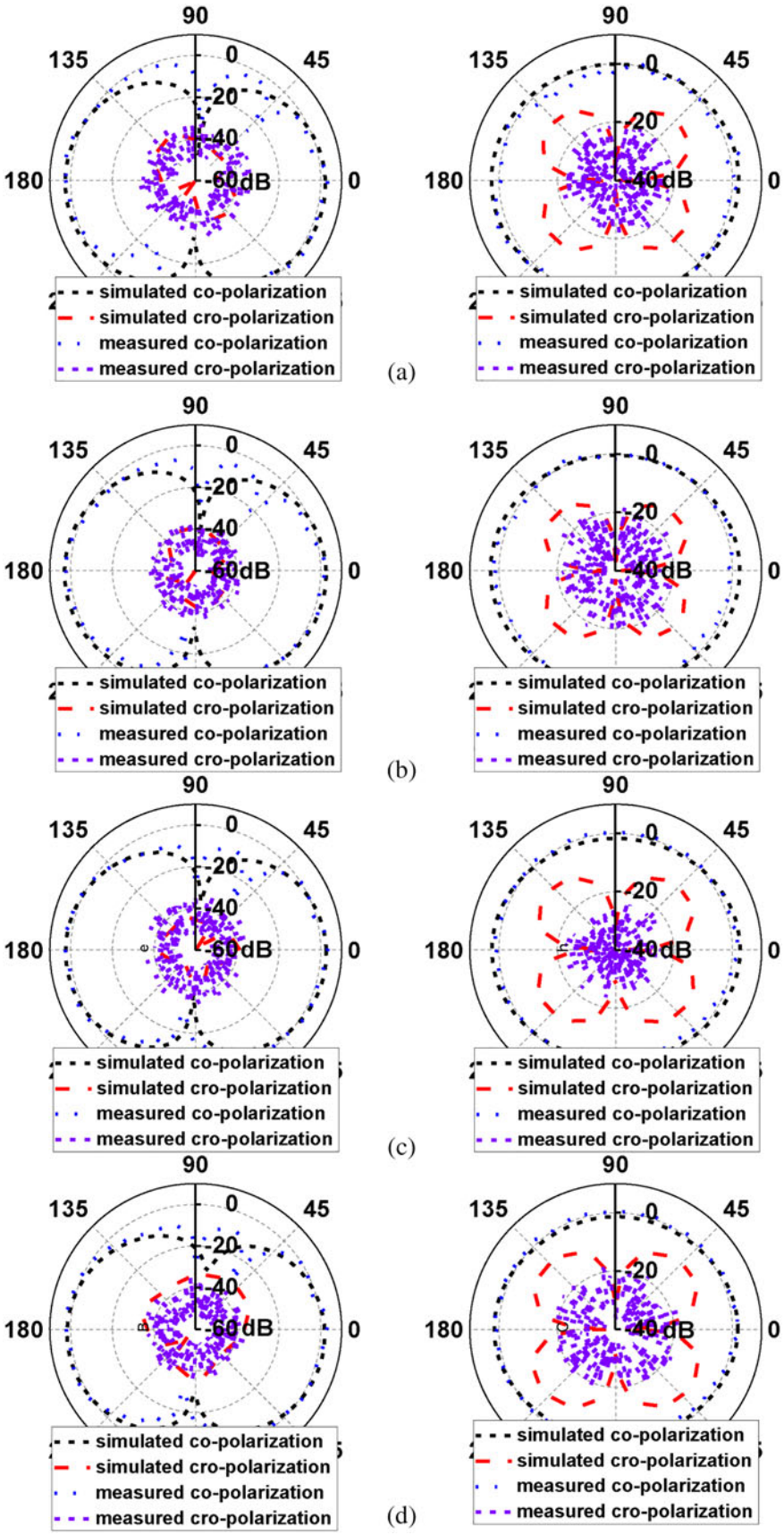

Fig. 8. Measured results of the band-notched monopole antenna with meta-surfaces. Measured E-plane (left) and H-plane (right) radiation patterns of (a) monopole antennas at 4 GHz with (b) single-band notched meta-surface at 4 GHz, (c) dual-band notched meta-surface at 4.5 GHz, and (d) tri-band notched meta-surface at 4.5 GHz.

https://doi.org/10.1017/S1759078722000873 Published online by Cambridge University Press

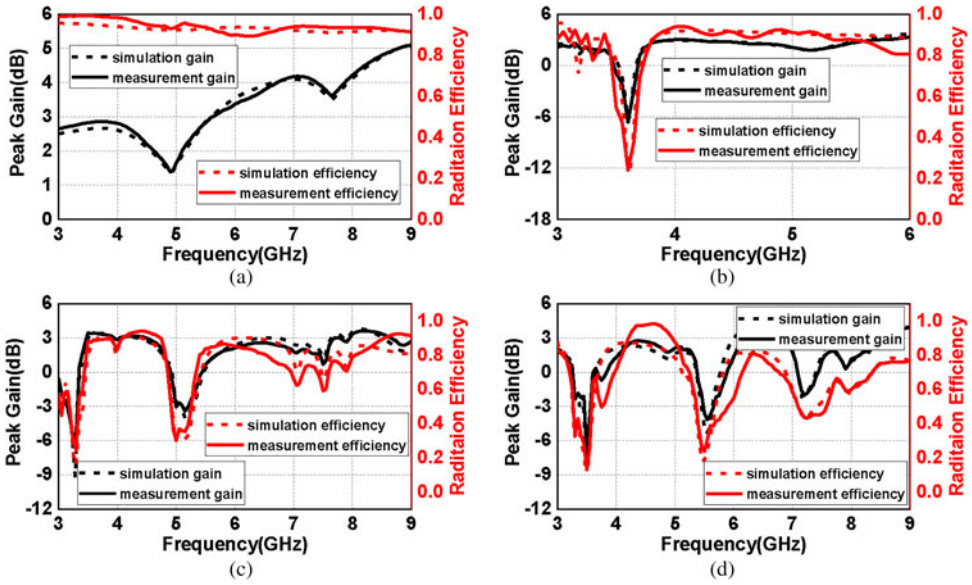

Fig. 9. Simulated and Measured results of the antenna gain variation with frequency. (a) Original monopole antennas. The band-notched antenna for (b) single-band, (c) dual-band and (d) tri-band.

Table 1. Performance comparisons between different band-notched antennas

Reference	Dimension (mm^2)	Bandwith (GHz)	Electrical size (λ_g^2)	Notched band	Notch technique	Hurting original antenna
[1]	70×70	3.8–8.3	1.48×1.48	Single	Carving slot	Yes
[4]	40×30	2.85–11.52	0.56×0.43	Quadruple	Carving slot	Yes
[6]	38×40	2.85–12.0	0.53×0.56	Six	Parasitic strip	Yes
[10]	32×14	3–12	0.67×0.29	Dual	Parasitic strip	Yes
[14]	32×27	2.98–10.76	0.68×0.58	Single	T-shaped stub	Yes
Proposed antenna	50×44	3–9	1.04×0.84	Single/ dual/ triple	Meta-surface	No

quite well with the simulation results. Such experimental results of band-notched monopole antennas further verify our designs and fulfill the initial proposal of using replaceable meta-surfaces to realize the reconfigurable band-notched monopole antennas. We test the radiation performance of the monopole antenna and the band-notched monopole antenna with meta-surfaces. Figure 8 demonstrates the radiation characteristics and we can observe that the radiation patterns of band-notched monopole antennas at un-notched frequencies are scarcely deteriorated when meta-surfaces are added. We can observe the ripples in the measured cross-polarized components. This is mainly attributed to the cross-polarization component amplitude that is small resulting in a low signal-noise ratio (SNR) during the antenna test process, thus the interference of noise in the measurement leads to poor cross-polarization component measurement results and produces the ripples. In addition, we simulate and measure the realized peak gain and efficiency of the proposed band-notched antenna as shown in Fig. 9 and both simulation and measurement results demonstrate that the proposed antenna achieved a good peak gain and radiation efficiency except notched bands. At notched bands the gain and radiation efficiency decrease drastically, which indicate the effects of the meta-surface.

The detailed comparisons with the previous publications concerning band-notched antennas are demonstrated in Table 1, where λ_g is the wavelength in the substrate at the minimum operating frequency. Compared with previous publications of band-notched antennas, our proposed band-notched monopole antenna implements the band-notched characteristics by attaching different meta-surfaces on the back of the antenna and demonstrates that the band-notched properties are changeable without compromising the original structure of the antenna.

Conclusion

A compact low profile microstrip planar UWB monopole antenna with meta-surface is presented. Through simply attaching different meta-surfaces on the back of the antenna, the dual-band notched properties around 3.3/5.15 GHz are shown to be changeable without destroying the original structure of the antenna. In addition, by adjusting the number and structure of SRR rings in the meta-surface, we extend our design into the single-band and tri-band notched monopole antenna. Both simulation and measurement results demonstrate that our proposed design can obtain significant notched performances for the desired bands, while maintaining the

https://doi.org/10.1017/S1759078722000873 Published online by Cambridge University Press

good radiations at the un-notched frequencies, hence is suitable for UWB wireless communication applications.

Acknowledgements. The experiments and tests done in this paper are carried out with the support of Aeronautic Remote Sensing System, China's Large research infrastructures. We are thankful for their support.

References

1. **B Mohamadzade, RBVB Simorangkir, RM Hashmi, Y Chao-Oger, M Zhadobov and R Sauleau** (2020) A conformal band-notched ultrawideband antenna with monopole-like radiation characteristics. *IEEE Antennas and Wireless Propagation Letters* **19**, 203–207.
2. **W Wu, B Yuan and A Wu** (2018) A quad-element UWB-MIMO antenna with band-notch and reduced mutual coupling based on EBG structures. *International Journal of Antennas and Propagation* **2018**, 8490740.
3. **B Feng, KL Chung, J Lai and Q Zeng** (2019) A conformal magneto-electric dipole antenna with wide H-plane and band-notch radiation characteristics for sub-6-GHz 5G base-station. *IEEE Access* **7**, 17469–17479.
4. **MJ Jeong, N Hussain, H Bong, JW Park, KS Shin, SW Lee, SYR Hee and N Kim** (2020) Ultrawideband microstrip patch antenna with quadruple band notch characteristic using negative permittivity unit cells. *Microwave and Optical Technology Letters* **62**, 816–824.
5. **Q Zhu and S Jiang** (2020) A compact flexible fractal ultra-wideband antenna with band notch characteristic. *Microwave and Optical Technology Letters* **63**, 895–901.
6. **S Luo, Y Chen, D Wang, Y Liao and Y Li** (2020) A monopole UWB antenna with sextuple band-notched based on SRRs and U-shaped parasitic strips. *AEU-International Journal of Electronics and Communications* **120**, 1434–8411.
7. **I Suriya and R Anbazhagan** (2019) Inverted-A based UWB MIMO antenna with triple-band notch and improved isolation for WBAN applications. *AEU-International Journal of Electronics and Communications* **99**, 25–33.
8. **K Srivastava, A Kumar, BK Kanaujia, S Dwari and S Kumar** (2019) A CPW-fed UWB MIMO antenna with integrated GSM band and dual band notches. *International Journal of RF and Microwave Computer-Aided Engineering* **29**, e21433.
9. **A Ghosh, T Mandal and S Das** (2019) Design and analysis of triple notch ultrawideband antenna using single slotted electromagnetic bandgap inspired structures. *Journal of Electromagnetic Waves and Applications* **33**, 1391–1405.
10. **A Gorai and R GHatak** (2019) Multimode resonator-assisted dual band notch UWB antenna with additional Bluetooth resonance characteristics.. *IET Microwaves, Antenna & Propagation* **13**, 1854–1859.
11. **AY Siddique, R Azim and M Islam** (2019) Compact planar ultra-wideband antenna with dual notched band for WiMAX and WLAN. *International Journal of Microwave and Wireless Technologies* **11**, 711–718.
12. **B Feng, L Li, J Cheng and C Sim** (2019) A dual-band dual-polarized stacked microstrip antenna with high-isolation and band-notch characteristics for 5G microcell communications. *IEEE Transactions on Antennas and Propagation* **67**, 4506–4516.
13. **R Azim and MT Islam** (2016) Ultra-wideband planar antenna with notched bands at 3.5/5.5 GHz. *ACES Journal* **31**, 388–395.
14. **R Azim, MT Islam and AT Mobashsher** (2014) Dual band-notch UWB antenna with single tri-arm resonator. *IEEE Antennas and Wireless Propagation Letters* **13**, 670–673.
15. **SU Rahman, Q Cao, Y Wang and H Ullah** (2019) Design of wideband antenna with band notch characteristics based on single notching element. *International Journal of RF and Microwave Computer-Aided Engineering* **29**, e21541.
16. **P Ranjan and A Kumar** (2021) Circularly polarized ultra-wide band filtering antenna with controllable band-notch for wireless communication system. *AEU-International Journal of Electronics and Communications* **135**, 153738.
17. **R Azim, MT Islam and AT Mobashsher** (2013) Design of a dual band-notch UWB slot antenna by means of simple parasitic slits. *IEEE Antennas and Wireless Propagation Letters* **12**, 1412–1415.
18. **AKMAH Siddique, R Azim and MT Islam** (2019) Compact planar ultra-wideband antenna with dual notched band for WiMAX and WLAN. *International Journal of Microwave and Wireless Technologies* **11**, 711–718.
19. **R Selvaraju, MH Jamaluddin, MR Kamarudin, J Nasir and MH Dahri** (2018) Mutual coupling reduction and pattern error correction in a 5G beamforming linear array using CSRR. *IEEE Access* **6**, 65922–65934.
20. **Z Wani and D Kumar** (2017) Dual-band-notched antenna for UWB MIMO applications. *International Journal of Microwave and Wireless Technologies* **9**, 381–386.
21. **A Habashi, J Nourinia and C Ghobadi** (2010) Mutual coupling reduction between very closely spaced patch antennas using low-profile folded split-ring resonators (FSRRs). *IEEE Antennas and Wireless Propagation Letters* **10**, 862–865.
22. **X Tan, W Wang, Y Wu, Y Liu and AA Kishk** (2019) Enhancing isolation in dual-band meander-line multiple antenna by employing split EBG structure. *IEEE Transactions on Antennas and Propagation* **67**, 2769–2774.
23. **M Abdalla, A Al-Mohamadi and I Mohamed** (2019) A miniaturized dual band EBG unit cell for UWB antennas with high selective notching. *International Journal of Microwave and Wireless Technologies* **11**, 1035–1043.
24. **C Singh and G Kumawat** (2020) A compact rectangular ultra-wideband microstrip patch antenna with double band notch feature at Wi-Max and WLAN. *Wireless Personal Communications* **114**, 2063–2077.
25. **A Yadav, RP Yadav and A Alphones** (2020) CPW fed triple band notched UWB antenna: slot width tuning. *Wireless Personal Communications* **111**, 2231–2245.
26. **R Marqués, F Medina and R Rafii-El-Idrissi** (2002) Role of bianisotropy in negative permeability and left-handed metamaterials. *Physical Review B* **65**, 144440–144446.
27. **K Fertas, F Ghanem, A Azrar and R Aksas** (2020) UWB antenna with sweeping dual notch based on metamaterial SRR fictive rotation. *Microwave and Optical Technology Letters* **62**, 956–963.
28. **M Rahman, WT Khan and M Imran** (2018) Penta-notched UWB antenna with sharp frequency edge selectivity using combination of SRR, CSRR, and DGS, AEU-International. *Journal of Electronics and Communications* **92**, 116–122.

Jinbiao Zhu received the M.D. degree from Tsinghua University, Beijing, China, in 2008. He is a professor of engineering, with Aerospace Information Research Institute, Chinese Academy of Sciences. He is engaged in the airborne remote sensing technologies and applications.

Wen Jiang received the Bachelor's degree and the Master's degree from Information Engineering University, Zhengzhou, China, in 1994 and 1997, and received her Ph.D. degree at Northwestern Polytechnical University, Xi'an, China, in 2009. She is currently a professor in School of Electronics & Information, Northwestern Polytechnical University. Her main research interests include multisource information fusion and artificial intelligence with uncertainty.

Yuquan Liu received the M.S. degree from Beijing Institute of Technology in 2009. He is a senior engineer with Aerospace Information Research Institute, Chinese Academy of Sciences. He is engaged in the airborne remote sensing technologies.

https://doi.org/10.1017/S1759078722000873 Published online by Cambridge University Press

Pengyu Yin received the B.E. degree from Harbin Engineering University in 2017 and the M.S. degree in engineering from Beijing University of Posts and Telecommunications in 2021. He is currently working at the Airborne Remote Sensing Center, AIRCAS, where he mainly studies the application of artificial intelligence in the field of remote sensing.

Lili Guo received her Master's degree in 2010 from Beihang University and had worked as an engineer in Airborne Remote Sensing Center, Chinese Academy of Sciences. She currently serves in the International Research Center of Big Data for Sustainable Development Goals and is now focusing on adapting Big Earth Data to meet the SDGs assessment, as well as providing education and training to developing countries for enhanced capacity building.

https://doi.org/10.1017/S1759078722000873 Published online by Cambridge University Press